Article:
Dembelova, T., Badmaev, B., Mashanov, A. et al. (2026) Viscoelastic properties of organosilicon fluid interlayer at low-frequency shear deformations. Fluids, 11 (1). 25. ISSN: 2311-5521

https://doi.org/10.3390/fluids11010025

fluids

MDPI

Article

Viscoelastic Properties of Organosilicon Fluid Interlayer at Low-Frequency Shear Deformations

Tuyana Dembelova [1,2,*], Badma Badmaev [1], Aleksandr Mashanov [1], Dari Dembelova [1], Michael I. Ojovan [3,4,*] and Migmar Darmaev [1,2]

[1] Institute of Physical Materials Science of the Siberian Branch of the Russian Academy of Sciences, 670047 Ulan-Ude, Russia; bbbadmaev@mail.ru (B.B.); sasha-89asd@mail.ru (A.M.); dembelovadari@gmail.com (D.D.); darmaev@bsu.ru (M.D.)
[2] Laboratory of Physics of Disordered Systems, Banzarov Buryat State University, 670000 Ulan-Ude, Russia
[3] School of Chemical, Materials and Biological Engineering, The University of Sheffield, Sheffield S1 3JD, UK
[4] Department of Radiochemistry, Lomonosov Moscow State University, 119991 Moscow, Russia
* Correspondence: dembelova@ipms.bscnet.ru (T.D.); m.ojovan@sheffield.ac.uk (M.I.O.); Tel.: +44-788-389-1379 (M.I.O.)

Abstract

The present work explores the viscoelastic properties of a homologous series of organosilicon fluids (polymethylsiloxane fluids) using the acoustic resonant method at a frequency of shear vibrations of approximately 100 kHz. The resonant method is based on investigating the influence of additional binding forces on the resonant characteristics of the oscillatory system. The fluid under study was placed between a piezoelectric quartz crystal that performs tangential oscillations and a solid cover plate. Standing shear waves were established in the fluid. The thickness of the liquid layer was much smaller than the length of the shear wavelength, and low-amplitude deformations allowed for the determination of the complex shear modulus G^* in the linear region, where the shear modulus has a constant value. The studies demonstrated the presence of a viscoelastic relaxation process at the experimental frequency, which is several orders of magnitude lower than the known high-frequency relaxation in liquids. In this work, the relaxation frequency of the viscoelastic process in the studied fluids and the effective viscosity were calculated, and the lengths of the shear wave and the attenuation coefficients were determined.

Keywords: polymethylsiloxane; shear elasticity; mechanical loss tangent; viscosity; shear wave; relaxation

Academic Editor: D. Andrew S. Rees

Received: 1 December 2025
Revised: 9 January 2026
Accepted: 17 January 2026
Published: 19 January 2026

1. Introduction

Organosilicon fluids demonstrate remarkable thermal stability across broad temperature ranges, making them suitable for diverse applications including hydraulic and diffusion systems, heat transfer media, and liquid dielectrics, and their use in the biomedical field is known. Their implementation extends to instrument oils, lubricating greases, damping fluids, polishing compositions, paint and lacquer additives, and as base components for consistent lubricants [1–9] or polymer matrices for developing functional materials with tailored characteristics [10–12]. This extensive application spectrum underscores the importance of investigating the viscoelastic properties of these fluids.

One of the effective methods in this direction is the study of the reaction of a fluid to dynamic disturbances, for example, to a shear effect with a certain frequency. The shear elasticity of liquids is observed at high frequencies of 10^{10}–10^{12} Hz and is explained by the

diffuse mobility of individual particles. The frequency of transfers of liquid particles from one equilibrium position to another has exactly this order of magnitude. Liquid molecules do not have time to react to external effects of such frequencies and higher, and the liquid shows properties characteristic of solid bodies.

The first studies of liquids with shear deformations were for strongly viscous liquids [13,14]. The early works of Mason [15] are known; they detail the shear elasticity of viscous polymer liquids by impedance method. Many works [16–20] are devoted to the study of shear mechanical properties of viscous liquids at high (MHz) frequencies. At low frequencies, this phenomenon is observed primarily in viscous liquids or in liquids in a supercooled state. Barlow and Lamb [17,18] show that the viscoelastic behavior of a number of pure and polymeric liquids as a function of frequency and temperature is described by the Maxwell rheological model with one relaxation time. Low-frequency (10^5 Hz) shear elasticity in low-viscosity fluids was first detected in works [21,22]. Study of low-frequency viscoelastic behavior of fluids away from phase transitions is carried out in works [23–31]. These studies confirm that in fluids, along with the high-frequency process, there is a low-frequency viscoelastic relaxation process with a relaxation time exceeding classical estimates. It is likely that the collective effects caused by the interaction of large molecular groups play a key role in some cases. Therefore, the relaxation requires a coordinated movement of many particles, and the low-frequency shear elasticity of liquids may be related to their micro-heterogeneous structure.

This work investigates the viscoelastic characteristics of organosilicon fluids using acoustic resonance technique. Polymer fluids exhibit more complex structural organization compared to simple liquids, where collective intermolecular interactions are expected to play a significant role. New experimental data on viscoelastic relaxation in organosilicon fluids would provide valuable insights into the underlying mechanisms of low-frequency viscoelastic relaxation in liquid systems.

2. Materials and Methods

Polyorganosiloxane fluids are characterized by low glazing temperatures, good dielectric and hydrophobic properties, significant compressibility, and low surface tension coefficient. Their viscosity has low temperature dependence. The characteristics of the mechanics and rheology of these substances are due to the high flexibility of polymer siloxane chains [1]. For the studies, linear polymethylsiloxane fluids of PMS brand were used which have a linear structure $(CH_3)_3Si–O–[Si(CH_3)_2O]_n–Si(CH_3)_3$ and meet the requirements of GOST 13032-77 [32]. The numbers in the brand name indicate the viscosity of the PMS fluid in cSt.

A classic model combining the elastic and viscous properties of fluids is Maxwell series connection of a spring and damper. In this model, the total strain ε is the sum of the strains of the elastic and viscous elements. The stresses σ in both elements are identical, and the relationship between the stresses and strains of the material is:

$$\dot{\varepsilon} = \frac{\dot{\sigma}}{G_M} + \frac{\sigma}{\eta_M}, \quad (1)$$

where G_M is the shear modulus of the model and η_M is its viscosity. If the Maxwell element is loaded with a certain stress σ_0 and the strain is specified and does not change ($\varepsilon = \varepsilon_0$), then Equation (1) yields the stress relaxation law: at constant strain, the stress decays exponentially: $\sigma = \sigma_0 \exp(-t/\tau_M)$. The quantity τ_M characterizes the rate of stress decay and is called the relaxation time. If the stress σ in an element is constant, then the strain rate is also constant and the deformation is unlimited. As follows from Equation (1), the model describes irreversible deformation, i.e., in this model, steady-state flow $d\varepsilon/dt = \sigma/\eta_0$

with constant viscosity η_0 (a property of a Newtonian fluid) is possible. Therefore, the Maxwell model describes well liquids and amorphous materials under shear deformation at temperatures above the glass transition temperature.

The study of viscoelastic characteristics of liquid media is effectively carried out by means of dynamic methods, which provide for cyclic deformation of the liquid with a given frequency of shearing oscillations. When applying sinusoidal varying stress $\sigma = \sigma_0 \cos \omega t$, with a frequency of $\omega = 2\pi f$, the deformation also varies sinusoidally $\varepsilon = \varepsilon_0 \cos(\omega t - \theta)$, where θ is the phase shift between stress and deformation. In this case, the complex shear modulus $G^* = G' + iG''$ is considered. For the rheological model of a viscoelastic material proposed by Maxwell, the complex shear modulus G^* is expressed as follows:

$$G^* = G_M \frac{\omega^2 {\tau_M}^2}{1 + \omega^2 {\tau_M}^2} + i\omega \frac{\eta_M}{1 + \omega^2 {\tau_M}^2}. \quad (2)$$

The real part of Expression (2) $\mathrm{Re}G^* = G'(\omega)$ is called the dynamic modulus of elasticity for the frequency ω, or the storage modulus. $\mathrm{Im}G^* = G''(\omega)$ is the loss modulus. The quantity $\eta = G''/\omega$ plays the role of viscosity. Energy losses are characterized by the tangent of the angle of mechanical losses $\tan\theta = G''/G'$. Therefore, the higher the dissipation, the greater the angle θ. Maximum energy loss corresponds to peak G'' when force exposure time coincides with stress relaxation time τ_M. From Equation (2), it follows that at low frequencies ($\omega\tau << 1$) the medium behaves as a viscous liquid, and with increasing frequency the storage modulus begins to increase, and at very high frequencies ($\omega\tau >> 1$) the medium behaves like an elastic solid.

The low-frequency viscoelastic properties of polymethylsiloxane fluids are investigated by acoustic resonance method using a piezoelectric resonator [33–35]. This method covers a wide range of viscosities from 10^{-3} to 10^5 Pa·s and is applicable to liquid layers 1–100 μm thick. The piezoelectric crystal is fixed in the points of the nodal line and oscillates at the main resonance frequency, creating tangential displacements (see Figure 1). The liquid is applied onto one end of the horizontal surface of the piezoquartz and covered with a cover plate made of fused quartz. The cut of the X-18.5° crystal, which has a zero Poisson coefficient on the working surface, provides exclusively shear deformations in the liquid layer, forming in the layer standing shear waves propagating along the z-axis with wave equation:

$$\rho \frac{\partial^2 \xi(z,t)}{\partial t^2} = G^* \frac{\partial^2 \xi(z,t)}{\partial z^2}, \quad (3)$$

where the displacement of liquid particles ξ(z, t) along the x-axis is described by the expression $\xi(z,t) = A\exp[i(\omega t - \kappa z)]$.

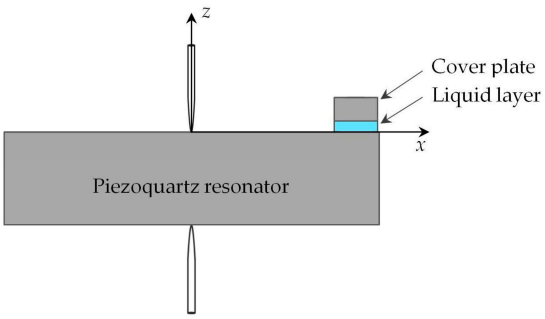

Figure 1. Piezoelectric quartz crystal with additional coupling.

The influence of the liquid in the layer is manifested in the change in resonance characteristics of the system. An increase in the resonance frequency relative to the free

quartz frequency indicates conservative forces in the liquid layer, while the dissipative forces of viscous friction cause a reduction in the resonance frequency of the system.

It is assumed that the liquid layer has viscoelastic properties, represented by the complex shift module $G^* = G' + iG''$. Then, the complex shift of the resonant frequency $\Delta\omega$ of the piezoelectric quartz crystal can be determined from the equality of the impedance of the liquid and the crystal and expressed as follows [33–35]:

$$\Delta\omega = \frac{2SG^*\kappa}{M\omega} \cdot \frac{1 + \cos(2\kappa H - \varphi)}{\sin(2\kappa H - \varphi)}, \tag{4}$$

where S is the contact area of the liquid and the quartz, H is the thickness of the liquid layer, M is the mass of the quartz, $\kappa = \beta - i\alpha$ is the complex wave number of the liquid, $\varphi = \varphi' + i\varphi''$ is the complex phase shift when the viscoelastic wave is reflected from the boundary of the liquid-cover plate. The real part of the complex phase shift φ' is equal to the phase difference between the incident and reflected waves at the liquid–cover plate interface. The imaginary part φ'' characterizes the additional attenuation caused by the loss of part of the wave energy transferred to the cover plate [33,34].

With the oscillation of the piezoquartz the cover plate of sufficient mass remains virtually immobile due to weak coupling through the liquid layer. So, there is no phase shift ($\varphi = 0$). This condition is well satisfied in the experiment and corresponds to the complete reflection of the wave energy. As a result, the real and imaginary parts of the complex shift of the linear frequency $\Delta f^* = \Delta f' + i\Delta f''$ take the following form [9]:

$$\Delta f' = \frac{SG'\beta}{4\pi^2 M f_0 \cos\theta} \cdot \frac{\sin 2\beta H - \tan\frac{\theta}{2}\sinh(2\beta H \cdot \tan\frac{\theta}{2})}{\cosh(2\beta H \cdot \tan\frac{\theta}{2}) - \cos 2\beta H}, \tag{5}$$

$$\Delta f'' = \frac{SG'\beta}{4\pi^2 M f_0 \cos\theta} \cdot \frac{\sin 2\beta H \cdot \tan\frac{\theta}{2} + \sinh(2\beta H \cdot \tan\frac{\theta}{2})}{\cosh(2\beta H \cdot \tan\frac{\theta}{2}) - \cos 2\beta H}, \tag{6}$$

where f_0 is the intrinsic resonance frequency of the quartz, $\tan(\theta/2) = \alpha/\beta$. These expressions show that for a viscoelastic fluid, the frequency shifts are functions of the layer thickness H, and with an increase in the latter, damped oscillations of the frequency shifts are observed.

According to Expressions (5) and (6), when the thickness H is much smaller than the wave length λ established within the liquid ($H << \lambda$), the complex shear modulus can be determined as:

$$G^* = \frac{4\pi^2 M f_0 \Delta f^* H}{S} \tag{7}$$

So the resonance frequency shift of piezoelectric quartz is inversely proportional to the thickness of the liquid layer. The $\Delta f''$ is determined as half of the change in the resonance curve width (Figure 1). The tangent of the loss angle is expressed as:

$$\tan\theta = G''/G' = \Delta f''/\Delta f'. \tag{8}$$

Consequently, for determining the complex shear modulus of liquids using thin layers ($H << \lambda$), it suffices to analyze the dependence of both real and imaginary frequency shifts on the reciprocal of layer thickness ($1/H$). The liquid layer thickness was determined using the interference method with an accuracy of 0.01 μm. A monochromatic beam was incident almost normally on the surface of the cover plate. When the wavelength λ of the light was smoothly varied by the monochromator, a periodic darkening of the reflected light was

observed when the light path difference in the liquid layer was equal to an odd number of half-wavelengths. The optical path δ of the light beam in the liquid layer was equal to:

$$\delta = 2nH\cos r + \frac{\lambda}{2},$$

where H is the thickness of the liquid layer in the gap, n is the refractive index of the liquid, and r is the angle of refraction of light in the liquid. From the condition of darkening of two adjacent interference fringes with λ_1 and λ_2, the following expression for determining the thickness H can be derived:

$$H = \frac{\lambda_1\lambda_2}{2n(\lambda_1 - \lambda_2)} \quad (9)$$

In the present experimental study, we employed an X-18.5° cut quartz resonator with a fundamental resonance frequency of 73.18 kHz, having a mass of 6.82 g. The cover plate contact area was 0.2 cm^2 and the mass was 0.2 g. For reproducibility of the measurement results, it is particularly important to thoroughly clean the working surfaces of the quartz and cover plate, as this promotes good wetting and prevents liquid slippage [35]. The overall relative error in determining the shear modulus of liquids using the acoustic resonance method was ~6%.

3. Results and Discussion

The shift of the oscillating system resonance frequency is influenced by an amplitude of the shear deformation [36,37]. When the amplitude of the oscillation increases, the resonance curves of the system deform. This indicates the non-linear nature of the shear elastic properties of the liquids [36–39]. The Fabry–Perot interferometer principle was used to determine the amplitude of the oscillation of piezoelectric quartz A. In this method, one of the mirrors is an optically polished end surface of a quartz resonator. The method is described in [38,39]. The interferometer's second mirror was mounted in a special frame with microscrews, which allowed it to be fixed plane-parallel to the end surface of the piezoquartz crystal. A Ne-He gas laser with a wavelength of 6328 Å was used as a monochromatic light source. As the piezoquartz vibrated, the distance between the interferometer mirrors was periodically varied. The interference pattern was observed in the focal plane of the lens and took the form of concentric rings, widening proportionally to the amplitude of the piezoelectric quartz crystal vibrations. As a result, the dependence of the oscillation amplitude on the voltage read from the piezoelectric quartz crystal was determined from the interference ring widening. The accuracy of amplitude measurements by this method is quite high. For example, with small oscillations of the piezocrystal, a change in the output voltage of 1 mV corresponds to a change in amplitude of 1 Å.

Figure 2a shows normalized resonance curves for the free piezoquartz with resonance amplitude A_{res} and for the piezoquartz loaded with a PMS-100 fluid layer of thickness H = 2.1 μm at maximum amplitude A of 15 Å in both cases. Analysis of the graphs shows that the resonance frequency of the loaded quartz is higher than that of the free piezoquartz, which corresponds to a positive shift in the resonance frequency. At the same time, the resonance curve broadens, showing an increase in the system's damping. On the change in the width of the resonance curve, it is possible to obtain the imaginary shift of the resonance frequency $\Delta f''$, defined as half the change in the width of the resonance curve (Figure 2a). It should also be noted that the resonance curves of free and loaded piezoquartz are almost symmetrical, which indicates the lack of non-linearity of the shear properties of the liquid. Figure 2b shows resonance curves at different forcing force values corresponding to the maximum amplitude A of 15 and 65 Å. For ease of comparison, the amplitude of the curves

is also normalized to a unit. As can be seen from the figure, with increasing amplitude of oscillations up to 66 Å, the resonance curve deforms and acquires pronounced asymmetry.

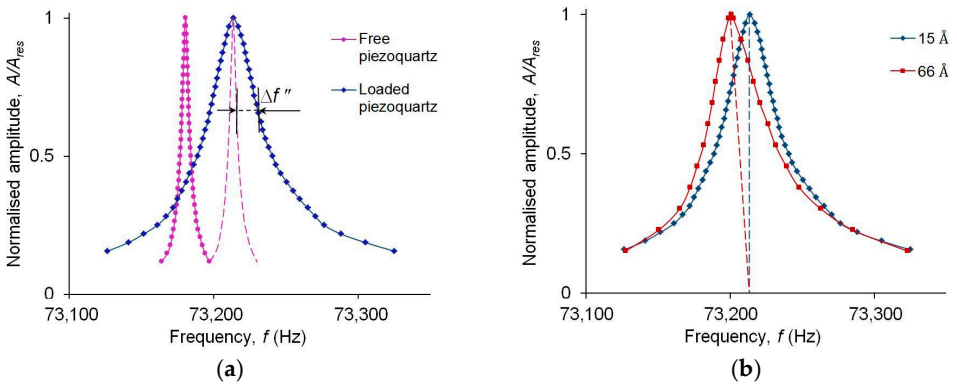

Figure 2. Resonance curves: (**a**) Free (unloaded) piezoquartz and loaded by PMS-100 fluid; (**b**) piezoquartz loaded by PMS-100 fluid with different maximum amplitudes, (H = 2.1 μm).

The A/H ratio between oscillation amplitude and liquid interlayer thickness can be used to measure angular deformation. The values of the storage modulus and loss modulus were obtained for PMS-100 at various shear strain values. Measurements were conducted at a thickness of 2.1 μm, when the resonant frequency shifts $\Delta f'$ and $\Delta f''$ were proportional to the inverse of the liquid layer thickness $1/H$. Figure 3 shows the theoretical dependence of the real and imaginary resonant frequency shifts on the inverse of the liquid layer thickness for PMS-100 using Expressions (5) and (6). As can be seen from the figure, the dependence is linear at small thicknesses; with increasing thickness, oscillations in the frequency shifts begin to be observed. Extrapolation of the linear dependences shows that both dependences tend to the origin.

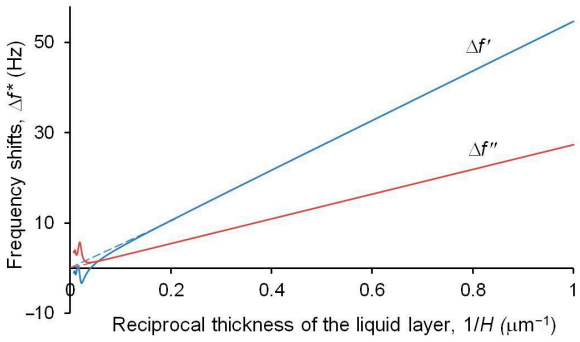

Figure 3. Dependence of the resonant frequency shifts on the inverse thickness of the liquid layer.

The values of the storage modulus and loss modulus for PMS-100 at various shear strain values are determined using Formula (7). Figure 4 shows the dependences of the components of the complex shear moduli G' and G'' on the square root of the strain $(A/H)^{1/2}$ for ease of analysis. The figure shows that at small angles of deformation the shear modulus remains constant. It indicates that linear elasticity is present. Assuming that the liquid has an equilibrium supramolecular structure with final strength and a relatively large relaxation period, it is obvious that at small angles of shift deformation the liquid structure remains unbroken. At a certain critical angle, the equilibrium structure begins to break down, which leads to changes in the viscoelastic properties of the liquid. Such behavior of viscoelastic properties, which is typical for dispersed systems, has been observed for other low-viscosity liquids at low-frequency shear deformations [36–39].

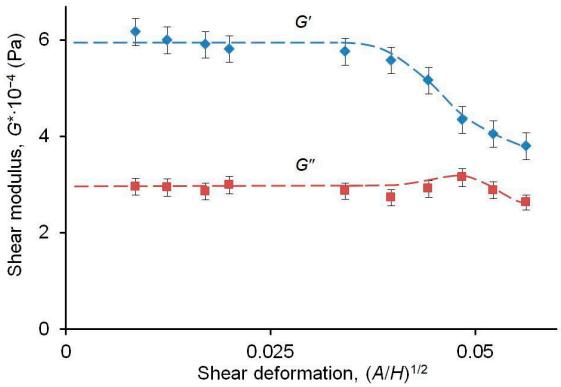

Figure 4. Dependences of the storage G' (1) and the loss G'' (2) moduli on the magnitude of shear deformation for PMS-100.

Measurements of the complex shift modulus of polymethylsiloxane fluids at small thicknesses of liquid interlayer in [40–42] were performed at small amplitudes when the resonant curve is symmetrical and corresponds to the linear elasticity region. The dependences of the resonant frequency shifts on $1/H$ were linear and converged to the origin. Thus, for all the studied liquids, a complex shear modulus was determined that was independent of the thickness of the liquid interlayer. In the study of even low-viscosity polymethylsiloxane liquids, the interlayer thickness was no less than 1 μm. It is possible that thinner layers of these liquids could exhibit a special boundary elasticity, which would lead to a sharp increase in the frequency shift with decreasing interlayer thickness. However, the existence of such elasticity was not observed in experiments. In [43–46], the influence of surface forces on the properties of thin liquid interlayers enclosed between solid surfaces was observed for thicknesses of the order of 1–100 nm. Figure 5 presents the dependencies of G' and tan θ on the logarithm of viscosity lgη for the homologous series of PMS fluids. As can be seen from the figure, the shear modulus increases by more than an order as the viscosity of the fluid increases. The tangent of the mechanical loss angle passes through a maximum as viscosity increases, but remaining less than unity.

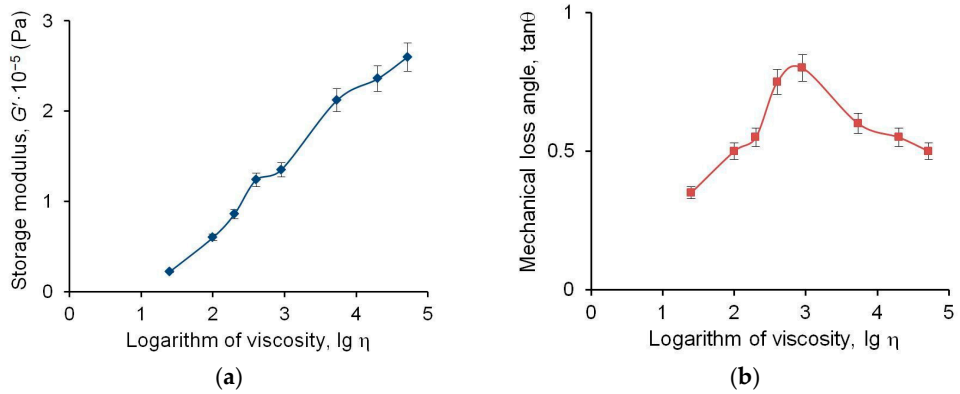

Figure 5. Dependence of viscoelastic parameters for a series of PMS fluids on the logarithm of viscosity lgη: (**a**) the storage modulus G'; (**b**) the tangent of the mechanical loss angle tan θ.

Assuming that the observed viscoelastic relaxation conforms to the Maxwell model, the frequency of the relaxation process $f_M = f_0 \cdot \tan\theta$ in PMS fluids should be below the frequency of the shear oscillations applied in the experiment. The relaxation frequency of PMS-100 fluid is equal to 37 kHz, and that of PMS-900 is 59.2 kHz. The relaxation frequency could have been directly determined experimentally at the given shear frequency for a fluid with a viscosity greater than 900 cSt but less than 5000 cSt, where tan θ would equal unity. Table 1 presents the calculated resonance frequency values f_M for all investigated PMS fluids

with density ρ, which have the storage modulus G' and mechanical loss tan θ, obtained at temperature t. The last column of the table shows the values of effective (apparent) viscosity, manifested in the experiment, calculated according to Maxwell rheological model using the following formula:

$$\eta_M = \frac{G'(1+\tan^2\theta)}{2\pi f_0 \tan\theta} \quad (10)$$

Table 1. Viscoelastic properties of series of PMS fluids.

Fluid	t, °C	$\rho \cdot 10^{-3}$, kg/m^3	$G' \cdot 10^{-5}$, Pa	tan θ	$f_M \cdot 10^{-3}$, Hz	η_M, Pa·s
PMS-25	24	0.94	0.22	0.35	25.90	0.15
PMS-100	23	0.97	0.60	0.50	37.00	0.32
PMS-200	22	0.97	0.86	0.55	40.70	0.44
PMS-400	23	0.98	1.24	0.75	55.50	0.55
PMS-900	22	0.98	1.35	0.80	59.20	0.59
PMS-5384	22	0.98	2.12	0.60	44.40	1.03
PMS-20,000	23	0.98	2.36	0.55	40.70	1.20
PMS-52,000	24	0.98	2.60	0.50	37.00	1.39

According to Table 1, the calculated viscosities η_M for low-viscous PMS fluids are significantly higher than nominal values. For instance, in the case of PMS-100 with a dynamic viscosity of 97 mPa·s, the effective viscosity η_M calculated using the Maxwell formula (10) is more than three times higher and is equal to 0.32 Pa·s. Figure 6, which plots the effective viscosity of PMS-100 against shear deformation correlating with the data of G^* presented in Figure 4, illustrates a shear-thinning behavior. The graph evidences that viscosity η_M decreases with increasing shear deformation and subsequently asymptotically approaches the standard (nominal) viscosity value. For high-viscosity PMS fluids (Table 1), the rise in nominal viscosity accompanying increased molecular weight reduces molecular diffusion and energy dissipation and so the Maxwell viscosity computed from rheological model proves lower than the standard value. The increase in nominal viscosity is due to the emerging entanglement network formed by mechanical intertwining of macromolecules with high molecular weights. A fluctuating entanglement network appears in macromolecules with a molecular weight M greater than the critical M_c, which for PMS liquids is 29,000 [47] and corresponds to PMS with viscosities greater than 1000 cSt. There are two molecular weight regions separated by a characteristic critical molecular weight value M_c for each polymer homologous series. In both regions, the dependence of viscosity on M can be represented by different power laws. This is probably why the tangent of the mechanical loss angle as a function of viscosity has a maximum; here, we see the manifestation of two types of interactions between molecules. It should be noted that the single-relaxation-time Maxwell model provides an approximate description of real liquid behavior. However, to explain the low-frequency shear elasticity, it can be assumed that at oscillations with small shear deformation, the liquid exhibits an equilibrium supramolecular structure. This may explain the observed high effective viscosities for low-viscosity PMS fluids and anomalously long relaxation times, where collective interactions of molecules become significant. In contrast, the nominal viscosity of PMS likely corresponds to a liquid with a broken spatial structure, corresponding to high-frequency relaxation.

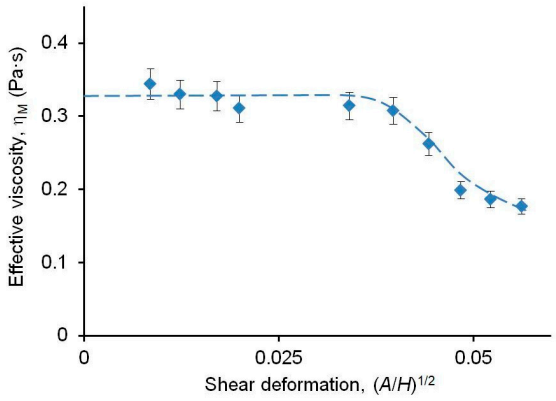

Figure 6. Effective viscosity vs magnitude of shear deformation for PMS-100.

Low-frequency relaxation in liquids can be compared with the slow λ-relaxation process in amorphous polymers, which is observed above their glass transition temperature and is explained by the breakdown and recovery of the micro-volume physical nodes of the molecular network [48,49]. The cluster model of liquids we are developing to explain the low-frequency shear elasticity assumes the existence in liquids and amorphous materials of fluctuating dynamic structural micro-heterogeneity clusters capable of formation and disintegrate over time [50–52]. Thus, the liquid represents micro-heterogeneous media consisting of ordered and unordered areas. The lifetime of clusters is significant due to the large number of bound molecules in the cluster and corresponds to a long relaxation time. Considering the relaxation time to be the reciprocal of the relaxation frequency, which corresponds to the maximum mechanical losses, study [51] established an exponential temperature dependence of the relaxation time and determined the activation energy of the low-frequency relaxation process for a polyethylsiloxane polymer fluid, $U \approx 26$ kJ/mol. Consequently, low-frequency viscoelastic relaxation in polymer (and possibly other) liquids can be classified as a low-activation process. It is noteworthy that the found activation energy of the low-frequency relaxation process in the polyethylsiloxane fluid coincides with the delocalization energy of the atom $\Delta\varepsilon \approx (20–25)$ kJ/mol in silicate glasses and their melts with siloxane bonds [51,53,54] in line with generic conclusions of relaxation character in amorphous materials [55–57]. In [33,50], the number of particles in a cluster was estimated within the framework of the cluster approach and the activation energy of the low-frequency viscoelastic process for Vaseline oil was determined. The values obtained for the number of particles in a Vaseline oil cluster were $z \approx 10^3$, and for the activation energy $U \approx 21.6$ kJ/mol, consistent with the elementary mechanism of this process, which is reduced to the detachment of a kinetic unit from the cluster. The obtained values of the activation energy in [33,50,51] are close to the energy of a hydrogen bond. Reliable determination of the activation energy of the low-frequency viscoelastic process under consideration, relaxation time, the sizes of ordered areas, and other parameters requires further studies of viscoelastic properties of PMS fluids at different frequencies and temperatures. Data on the tangent of the mechanical loss angle in a sufficiently wide temperature range at different frequencies will make it possible to apply methods of relaxation spectrometry of polymers [48,49] and calculate these important parameters of low-frequency viscoelastic relaxation in the frame of the cluster model of liquids.

If the liquid possesses shear elasticity and the tangent of the angle of mechanical losses is less than unit, then the distance at which the shear wave decays can be equal to several wavelengths, which enables the study of their propagation [52,58,59]. In [33,34,40–42], the lengths of shear waves λ and viscoelastic parameters G' and tan θ of some polymethylsiloxane and other liquids were experimentally determined using an ultrasonic interferometer on shear waves at a shear oscillation frequency of 74 kHz. The studies of shear wave

propagation indicate that low-frequency shear elasticity is a property of the liquid in bulk and is not related to boundary phenomena. However, the method for determining viscoelastic parameters based on shear wave propagation is well suited for studying only viscous liquids. To obtain a liquid thickness comparable to the wavelength, the overlay was rigidly fixed to a stationary platform with micrometer screws, which were used to regulate the thickness [34]. Due to the rigid fixation of the overlay, the normal component of piezoelectric quartz oscillations, which is always present in real crystals, begins to influence the experimental data. This causes additional compression and tension deformations in the liquid interlayer. In this case the mechanical properties in different parts of the liquid interlayer may turn out to be different, and the attenuation maxima are smoothed out. As the viscosity of the liquid increases, the influence of the normal component decreases but does not completely disappear. Therefore, some assumptions of the method in [33,34,40–42] give values of the shear modulus based on the shear wavelength somewhat lower than the values presented in Table 1. Comparison of the obtained data leads to the conclusion that the determination of the complex shear modulus of liquids by the resonance method at small layer thicknesses, when $H << \lambda$, is the most accurate. Using the data in Table 1 for calculations allows to obtain more accurate shear wave parameters.

From the theory of the acoustic resonance method for determining the complex shear modulus of liquids, the wavelength λ is determined by the position of the maximum attenuation values [9,33,34]:

$$H = \frac{\lambda}{2}n. \quad (11)$$

Accordingly, the first maximum of attenuation is observed at a thickness of the liquid layer equal to $\lambda/2$. Figure 7 shows the dependencies of the components of the resonance frequency shifts $\Delta f'$ and $\Delta f''$ on the layer thickness H for PMS-400, calculated using Equations (5) and (6) using the experimentally obtained data G' and tan θ from Table 1. According to Expression (11), the shear wavelength λ in PMS-400 is determined from the curve dependence of $\Delta f''(H)$ and it is equal to 180 μm, while experimental measurements give a value of 160 μm [41,42].

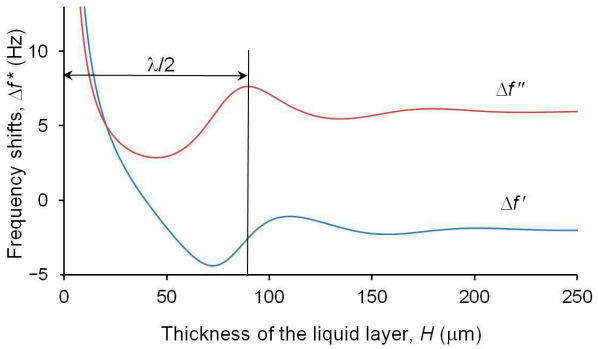

Figure 7. Influence of the thickness of the PMS-400 layer on the change in the components of the complex frequency shift.

To refine the wavelength data for the homologous series of PMS fluids, the $\Delta f''(H)$ dependences were calculated using viscoelastic parameters obtained by the method at $H << \lambda$. Figure 8 presents similar curves for the imaginary shift of the resonance frequency as a function of thickness for a series of PMS fluids. As can be seen from the figure, increasing thickness leads to damped oscillations of $\Delta f''$, and the length of the shear waves increases with increasing fluid viscosity. Consequently, the wave penetration depth also increases, which is equal to the distance at which the wave amplitude decreases by a factor of e.

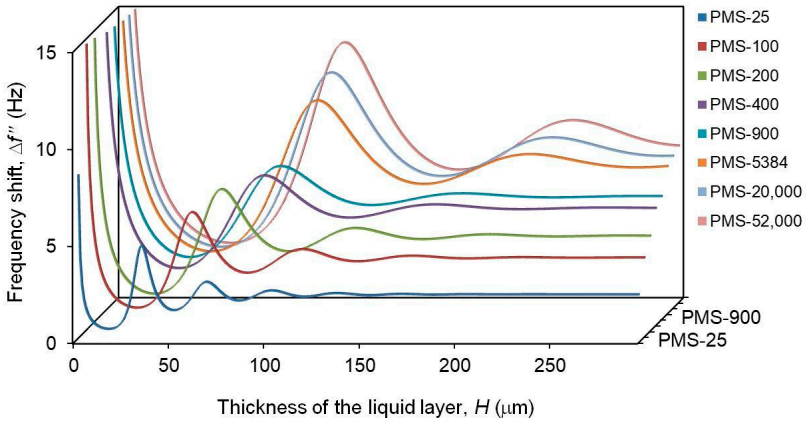

Figure 8. Imaginary component of frequency shift $\Delta f''$ vs. thickness of the layer H for PMS fluids.

Table 2 presents the shear wave lengths for PMS fluids obtained using Expression (9) from the positions of the first maximum of the $\Delta f''(H)$ dependences shown in Figure 8. It turns out that the obtained λ exceeds the experimental values in [33,34,40–42] by approximately 10–12%, which may be important for modeling the rheological properties of fluids and influence their subsequent practical application. The last column of Table 2 shows the attenuation coefficients α, calculated using Expression (12) [58]. It is evident from the table that the attenuation coefficients decrease with increasing viscosity of PMS fluids.

$$\alpha = \frac{2\pi}{\lambda} \tan \theta/2 \quad (12)$$

Table 2. Acoustic characteristics of a shear wave in PMS fluids.

Liquid	λ, μm	α, cm^{-1}
PMS-25	68	156.9
PMS-100	116	127.8
PMS-200	140	115.2
PMS-400	180	116.3
PMS-900	190	115.9
PMS-5384	222	78.4
PMS-20,000	232	69.5
PMS-52,000	240	61.8

With increasing molecular weight of the PMS fluid in the homologous series, the shear wavelength increases, while the attenuation coefficients decrease. This indicates a change in the liquid structure. It is probable that the greater the molecular weight of the polymer, the larger the sizes of the ordered areas in the liquid become. Larger associates are formed due to the increase in possible intermolecular and intramolecular interactions, caused, for example, by hydrogen bonds. The attenuation of the shear wave amplitude with increasing molecular weight is associated with energy dissipation and indicates that the elastic response begins to increasingly dominate the viscous response. This correlates with the effective viscosity data for high-viscosity PMS fluids compared to the nominal viscosity in Table 1. In addition, as shown in Figure 5a, the shear modulus also increases, and the fluid exhibits more pronounced elastic properties inherent to solids with increasing molecular weight.

4. Conclusions

In the work, a study of viscoelastic properties of polymethylsiloxane fluids was carried out in dynamic mode using an acoustic resonance method. It was shown that the relaxation time of the observed viscoelastic relaxation process is much longer than the settled lifetime of individual liquid particles and, according to the cluster model of the fluid, is due to microheterogeneity of structure. The change in their physical–mechanical and viscous properties depending on the amplitude of shear oscillations was shown. Values of shear wave lengths and attenuation factors were determined. Changes in wavelengths and attenuation coefficients with increasing molecular weight of the homologue indicate changes in the structure of the liquid, the formation of larger clusters in the liquid, which is manifested in an increase in the elastic response and a decrease in dissipative effects.

The results obtained are of considerable practical value due to the wide use of polymethylsiloxane fluids in modern technologies. The data on the viscoelastic properties of PMS can be used to develop science-based approaches for creating new organosilicon materials and composite materials based on them with nano-fillers for application in various fields of technology and technology, in particular, to create high-performance lubricants for precision instruments. Data on shear wave and attenuation parameters can be of practical importance for the selection of optimal polymethylsiloxane fluids used in measurement technology such as damping and working fluids, and taking into account their vibration and acoustic characteristics can contribute to improving the efficiency of devices.

Author Contributions: Conceptualization, T.D. and B.B.; methodology, B.B. and T.D.; validation, T.D. and B.B.; formal analysis, T.D., D.D.; investigation, T.D., A.M., M.D. and B.B.; resources, B.B.; writing—original draft preparation, T.D.; writing—review and editing, T.D., B.B. and M.I.O.; supervision, B.B.; project administration, T.D. All authors have read and agreed to the published version of the manuscript.

Funding: The work was performed under the IPMS SB RAS state budget project FWSF–2024–0012.

Institutional Review Board Statement: Not applicable.

Informed Consent Statement: Not applicable.

Data Availability Statement: The data presented in this study are available on request from the corresponding authors.

Conflicts of Interest: The authors declare no conflicts of interest.

References

1. Sobolevsky, M.V.; Muzovskaya, O.A.; Popeleva, G.S. *Properties and Applications of Organosilicone Products*; Khimiya: Moscow, Russia, 1975; pp. 88–110.
2. Teixeira, I.; Castro, I.; Carvalho, V.; Rodrigues, C.; Souza, A.; Lima, R.; Teixeira, S.; Ribeiro, J. Polydimethylsiloxane mechanical properties: A systematic review. *AIMS Mater. Sci.* **2021**, *8*, 952–973. [CrossRef]
3. Zolper, T.; Li, Z.; Chen, C.; Jungk, M.; Marks, T.; Chung, Y.-W.; Wang, Q. Lubrication Properties of Polyalphaolefin and Polysiloxane Lubricants: Molecular Structure—Tribology Relationships. *Tribol. Lett.* **2012**, *48*, 355–365. [CrossRef]
4. Zhiheng, W.; Dehua, T.; Xuejin, S.; Xiaoyang, C. Study on a new type of lubricating oil for miniature bearing operating at ultra-low temperature. *China Pet. Process. Petrochem. Technol.* **2018**, *20*, 93–100. Available online: http://carbonandhydrogen.com/EN/Y2018/V20/I1/93 (accessed on 10 November 2025).
5. Niu, R.; Gong, J.; Xu, D.; Tang, T.; Sun, Z.-Y. Rheological properties of ginger-like amorphous carbon filled silicon oil suspensions. *Colloids Surf. A Physicochem. Eng. Asp.* **2014**, *444*, 120–128. [CrossRef]
6. Chichester, C.W. *Development of High Service Temperature Fluids*; SAE Technical Paper 2016-01-0484; SAE International: Warrendale, PA, USA, 2016. [CrossRef]
7. Wu, W.; Li, P.; Wang, X.; Zhang, B. Grafting of thermotropic fluorinated mesogens on polysiloxane to improve the processability of linear low-density polyethylene. *RSC Adv.* **2022**, *12*, 12463–12470. [CrossRef] [PubMed]

8. Guan, X.; Cao, B.; Cai, J.; Ye, Z.; Lu, X.; Huang, H.; Liu, S.; Zhao, J. Design and synthesis of Polysiloxane based side chain liquid crystal polymer for improving the processability and toughness of Magnesium hydrate/linear low-density Polyethylene composites. *Polymers* **2020**, *12*, 911. [CrossRef] [PubMed]
9. Dembelova, T.; Badmaev, B.; Makarova, D.; Mashanov, A.; Mishigdorzhiyn, U. Rheological and tribological study of polyethylsiloxane with SiO_2 nanoparticles additive. *Lubricants* **2023**, *11*, 9. [CrossRef]
10. Chimytov, T.A.; Nomoev, A.V.; Kalashnikov, S.V.; Ojovan, M.I.; Darmaev, M.V.; Mashanov, A.A.; Kim, T.B. Observation of memory effects in 5CB/PVAc liquid crystal-polymer composites. *AIMS Mater. Sci.* **2025**, *12*, 744–754. [CrossRef]
11. Han, J.; Tang, Y.; Yue, L.; Ma, X.; Jia, H.; Liu, N.; Bai, P.; Meng, Y.; Tian, Y. Tribological behavior of polydiethylsiloxane (PDES) in a Si_3N_4 and M50 system under low temperatures from −80 to 25 °C. *Lubricants* **2024**, *12*, 176. [CrossRef]
12. Yue, L.; Meng, Y.; Lee, E.; Bai, P.; Pan, Y.; Wei, P.; Cheng, J.; Meng, Y.; Tian, Y. Effect of phosphide additives on the tribological properties of polyethylsiloxane (PES) in Si_3N_4 and M50 system. *Ind. Lubr. Tribol.* **2024**, *76*, 1025–1035. [CrossRef]
13. Volarovich, M.P.; Derjaguin, B.V.; Leontieva, A.A. Measurement of the shear modulus of vitreous systems in the softening interval. *Acta Phys. Chem.* **1936**, *8*, 479–485.
14. Kornfeld, M. Elastic and strength properties of liquids. *J. Exp. Theor. Phys.* **1943**, *13*, 116–122.
15. Mason, W.P. Measurement of the viscosity and shear elasticity of Liquids by means of a torsionally vibrating crystal. *Trans. ASME* **1947**, *69*, 359–370. [CrossRef]
16. McSkimin, H.J.; Andreatch, P. Measurement of Dynamic shear Impedance of low viscosity Liquids at Ultrasonic Frequencies. *J. Acoust. Soc. Am.* **1967**, *42*, 248–252. [CrossRef]
17. Barlow, A.J.; Lamb, J.; Matheson, A.J. Viscous behaviour of supercooled liquids. *Proc. R. Soc. Lond. Ser. A Math. Phys. Sci.* **1966**, *292*, 322–342. [CrossRef]
18. Lamb, J. Mechanical retardation and relaxation in liquids. *Rheol. Acta* **1971**, *12*, 438–448. [CrossRef]
19. Fritz, G.; Pechhold, W.; Willenbacher, N.; Wagner, N.J. Characterizing complex fluids with high frequency rheology using torsional resonators at multiple frequencies. *J. Rheol.* **2003**, *47*, 303–319. [CrossRef]
20. Yoshizaki, H. Measurement of viscoelastic properties of polymer solution by tortional crystals. *Polym. J.* **1993**, *25*, 553–559. [CrossRef]
21. Bazaron, U.B.; Derjaguin, B.V.; Bulgadaev, A.V. On shear elasticity of boundary layers of liquids. *Dokl. Akad. Nauk. SSSR* **1965**, *160*, 799–803.
22. Bazaron, U.B.; Derjaguin, B.V.; Bulgadaev, A.V. Measurement of the shear elasticity of fluids and their boundary layers by a resonance method. *J. Exp. Theor. Phys.* **1966**, *24*, 645–653.
23. Joseph, D.D.; Riccius, O.; Arney, M. Shear waves speeds and elastic moduli for different liquids, Part II. Theory. *J. Fluid Mech.* **1986**, *171*, 309–338. [CrossRef]
24. Collin, D.; Martinoty, P. Dynamic macroscopic heterogeneities in a flexible linear polymer melt. *Physica A* **2003**, *320*, 235–248. [CrossRef]
25. Ohsawa, T.; Wada, Y. Acoustic relaxations in toluene and alcohols in the frequency range of 10 to 300 kHz measured by the resonance reverberation method. *Jpn. J. Appl. Phys.* **1969**, *8*, 411–420. [CrossRef]
26. Noirez, L.; Baroni, P. Identification of a low-frequency elastic behaviour in liquid water. *J. Phys. Condens. Matter* **2012**, *24*, 372101. [CrossRef] [PubMed]
27. Noirez, L.; Baroni, P. Identification of thermal shear bands in a low molecular weight polymer melt under oscillatory strain field. *Colloid Polym. Sci.* **2018**, *296*, 713–720. [CrossRef]
28. Zaccone, A.; Trachenko, K. Explaining the low-frequency shear elasticity of confined liquids. *Proc. Natl. Acad. Sci. USA* **2020**, *117*, 19653–19655. [CrossRef]
29. Kume, E.; Zaccone, A.; Noirez, L. Unexpected thermo-elastic effects in liquid glycerol by mechanical deformation. *Phys. Fluids* **2021**, *33*, 072007. [CrossRef]
30. Kayanattil, M.; Huang, Z.; Gitaric, D.; Epp, S.W. Rubber-like elasticity in laser-driven free surface flow of a Newtonian fluid. *Proc. Natl. Acad. Sci. USA* **2023**, *120*, e2301956120. [CrossRef] [PubMed]
31. Yamada, T.; Sakai, K. Observation of collision and oscillation of microdroplets with extremely large shear deformation. *Phys. Fluids* **2012**, *24*, 022103. [CrossRef]
32. STAR. Available online: https://star-pro.ru/gost/13032-77 (accessed on 10 November 2025).
33. Badmaev, B.B.; Dembelova, T.S.; Damdinov, B.B. *Viscoelastic Properties of Polymer Liquids*; Publisher of the Buryat Scientific Center, SB RAS: Ulan-Ude, Russia, 2013; 190p.
34. Badmaev, B.B.; Dembelova, T.S.; Makarova, D.N.; Gulgenov, C.Z. Ultrasonic Interferometer on Shear Waves in Liquids. *Russ. Phys. J.* **2020**, *62*, 1708–1715. [CrossRef]
35. Badmaev, B.; Dembelova, T.; Damdinov, B.; Makarova, D.; Budaev, O. Influence of surface wettability on the accuracy of measurement of fluid shear modulus. *Colloids Surf. A Physicochem. Eng. Asp.* **2011**, *383*, 90–94. [CrossRef]

36. Dembelova, T.S.; Badmaev, B.B.; Makarova, D.N.; Vershinina, Y.D. Nonlinear viscoelastic properties of nanosuspensions. *IOP Conf. Ser. Mater. Sci. Eng.* **2019**, *704*, 012005. [CrossRef]
37. Bazaron, U.B.; Derjaguin, B.V.; Zandanova, K.T.; Lamazhapova, K.D. Nonlinear properties of shear elasticity of liquids. *Zhurnal Fiz. Khimii* **1981**, *55*, 2812–2816.
38. Badmaev, B.B.; Dembelova, T.S.; Makarova, D.N.; Gulgenov, C.Z. Shear elasticity and strength of the liquid structure by an example of diethylene glycol. *Tech. Phys.* **2017**, *62*, 14–17. [CrossRef]
39. Derjaguin, B.V.; Bazaron, U.B.; Zandanova, K.T.; Budaev, O.R. The complex shear modulus of polymeric and small-molecule liquids. *Polymer* **1989**, *30*, 97–103. [CrossRef]
40. Badmaev, B.B.; Bazaron, U.B.; Derjaguin, B.V.; Budaev, O.R. Measurement of the shear elasticity of polymethylsiloxane liquids. *Physica B+C* **1983**, *122*, 241–245. [CrossRef]
41. Derjaguin, B.V.; Badmaev, B.B.; Bazaron, U.B.; Lamazhapova, K.D.; Budaev, O.R. Measurement of the low-frequency shear modulus of polymeric liquids. *Phys. Chem. Liq.* **1995**, *29*, 201–209. [CrossRef]
42. Badmaev, B.B.; Budaev, O.R.; Dembelova, T.S.; Damdinov, B.B. Shear elasticity of fluids at low frequent shear influence. *Ultrasonics* **2006**, *44*, e1491–1494. [CrossRef]
43. Churaev, N.V. Thin liquid layers. *Colloid J.* **1996**, *58*, 681–693.
44. Yamada, Y.; Ichii, T.; Utsunomiya, T.; Sugimura, H. Visualizing polymeric liquid/solid interfaces by atomic force microscopy utilizing quartz tuning fork sensors. *Jpn. J. Appl. Phys.* **2020**, *59*, SN1009. [CrossRef]
45. Wang, R.; Souilamas, M.; Esfandiar, A.; Fabregas, R.; Benaglia, S.; Nevison-Andrews, H.; Yang, Q.; Normansell, J.; Ares, P.; Ferrari, G.; et al. In-plane dielectric constant and conductivity of confined water. *Nature* **2025**, *646*, 606–610. [CrossRef]
46. Fumagalli, L.; Esfandiar, A.; Fabregas, R.; Hu, S.; Ares, P.; Janardanan, A.; Yang, Q.; Radha, B.; Taniguchi, T.; Watanabe, K.; et al. Anomalously low dielectric constant of confined water. *Science* **2018**, *360*, 1339–1342. [CrossRef]
47. Vinogradov, G.V.; Malkin, A.Y. *Rheology of Polymers*; Khimiya: Moscow, Russia, 1977; pp. 179–190.
48. Bartenev, G.M.; Sanditov, D.S. *Relaxation Processes in Glassy Systems*; Nauka: Novosibirsk, Russia, 1986; pp. 160–165.
49. Bartenev, G.M.; Barteneva, A.G. *Relaxation Properties of Polymers*; Khimiya: Moscow, Russia, 1992; pp. 130–140.
50. Badmaev, B.B.; Damdinov, B.B.; Dembelova, T.S. Viscoelastic relaxation in fluids. *Bull. Russ. Acad. Sci. Phys.* **2015**, *79*, 1301–1305. [CrossRef]
51. Dembelova, T.S.; Sanditov, D.S. Low-frequency viscoelastic relaxation in polymer liquids. *Bull. Buryat State Univ. Chem. Phys.* **2022**, *1*, 24–31. (In Russian) [CrossRef]
52. Isakovich, M.A.; Chaban, I.A. Propagation of sound in strongly viscous liquids. *Sov. Phys. JETP* **1966**, *23*, 893–905. Available online: http://www.jetp.ras.ru/cgi-bin/dn/e_023_05_0893.pdf (accessed on 10 November 2025).
53. Sanditov, D.S. Thermally induced low-temperature relaxation of plastic deformation in glassy organic polymers and silicate glasses. *Polym. Sci. Ser. A* **2007**, *49*, 549–557. [CrossRef]
54. Sanditov, D.S.; Ojovan, M.I. On relaxation nature of glass transition in amorphous materials. *Physica B* **2017**, *523*, 96–113. [CrossRef]
55. Schawe, J.E.K.; Hallavant, K.; Esposito, A.; Löffler, J.F.; Saiter-Fourcin, A. The Universality of Cooperative Fluctuations in Glass-Forming Supercooled Liquids. *J. Phys. Chem. Lett.* **2025**, *16*, 12255–12265. [CrossRef]
56. Ojovan, M.I.; Louzguine-Luzgin, D.V. Role of Structural Changes at Vitrification and Glass–Liquid Transition. *Materials* **2025**, *18*, 3886. [CrossRef]
57. Ojovan, M.I.; Tournier, R.F. On structural rearrangements near the glass transition temperature in amorphous silica. *Materials* **2021**, *14*, 5235. [CrossRef]
58. Philippoff, W. Relaxation in polymer solutions, polymer liquids and gels. In *Physical Acoustics. Properties of Polymers and Nonlinear Acoustics*; Mason, W.P., Ed.; Mir: Moscow, Russia, 1969; Volume II, Part B, pp. 9–109.
59. Torres, J.; Laloy-Borgna, G.; Rus, G.; Catheline, S. A phase transition approach to elucidate the propagation of shear waves in viscoelastic materials. *Appl. Phys. Lett.* **2023**, *122*, 223702. [CrossRef]